

# Analysis of disturbing effect of 3 kV DC supplied traction vehicles equipped with two-level and three-level VSI on railway signalling track circuits

M. STECZEK<sup>1\*</sup>, A. SZELAĞ<sup>2</sup>, D. CHATTERJEE<sup>3</sup>

<sup>1</sup>Lodz University of Technology, 116 Żeromskiego St., 90-924 Łódź, Poland

<sup>2</sup>Warsaw University of Technology, 1 Politechniki Sq., 00-661 Warsaw, Poland

<sup>3</sup>Jadavpur University, 188, Raja Subodh Chandra Mallick Road, Jadavpur, Kolkata, West Bengal 700032, Indie

**Abstract.** Electric traction vehicles cooperating with a 3kV DC traction system and equipped with drive systems based on voltage source inverters are the most significant sources of disturbances for a railway signalling system. Every traction vehicle to be authorised for operation on railway lines must fulfil the limits imposed on current harmonics magnitudes and those provided by railway operators. The solution introduced for prototypes of most modern traction drives is to replace the two-level inverters with three-level topology. Therefore, it is essential to establish the influence of the new solution on the railway signalling system. This paper presents a comparative analysis between simulation results delivered for two and three-level traction drive system regarding generation of disturbing current harmonics. Two types of VSI modulation techniques were taken under consideration: sinusoidal PWM (SPWM) and a new one, proposed by the authors, based on selective harmonic elimination (SHE). Furthermore, the authors presented application of one of the SHE based optimization techniques for shaping the EMU's (electric multiple unit) DC side input current harmonics spectrum in order to meet the required limits. The described technique is based on off-line generation of a set of solutions for each of the VSI operating points and selection of the best solution for the assumed criteria. The applied simulation models and the concept of SHE control were verified in a laboratory by means of a low-power drive stand. Using the three-level inverter in traction drives system results in less current harmonics than using two-level topology without modification of the modulation technique. Thus, it does not guarantee fulfilling all limits assumed in this paper. The proposed modulation technique allows for fulfilling the limits, and the technical implementation of the proposed technique in a traction drive system will be considered in future studies.

**Key words:** voltage source inverters, traction vehicle, compatibility, harmonics, harmonics elimination.

## 1. Introduction

Multilevel inverters, promising solutions for AC drives in traction applications, are constantly under development. However, in high power DC supplied traction vehicles the two-level voltage source inverters (VSI) are used as a standard solution. For instance, most Polish manufacturers of modern rolling stock still use the two-level inverters which require, due to compatibility requirements [1], bulky input filters in order to reduce harmonics in a vehicle's current taken from catenary (catenary current –  $I_{cat}$ ). Therefore, an analysis of possible ways of reducing the level of distortions generated by vehicles by applying multilevel converters is a current issue for rolling stock manufacturers [2, 3].

Multilevel inverters constitute a novel solution for railway traction applications. For that reason, it is worth providing a comparative analysis between the two- and three-level inverters to verify the advantages. It is known that an output voltage waveform generated by the three-level VSI is characterised by a lower THD value than the two-level one [4, 5], considering the same number of switching per cycle. There-

fore, it generates less current and torque harmonics, resulting in lesser power losses and increased life-time of the drive. Another problem is developing a control strategy to make this type of inverters suitable for operation in traction and industrial environment. The application of a direct torque control (DTC) strategy for this purpose was presented in [6].

The preferred topology of the three-level inverter for traction application seems to be the neutral point clamped NPC topology (Fig. 3b). This solution requires an additional modification of modulation to eliminate the neutral point voltage fluctuations [5, 7, 8].

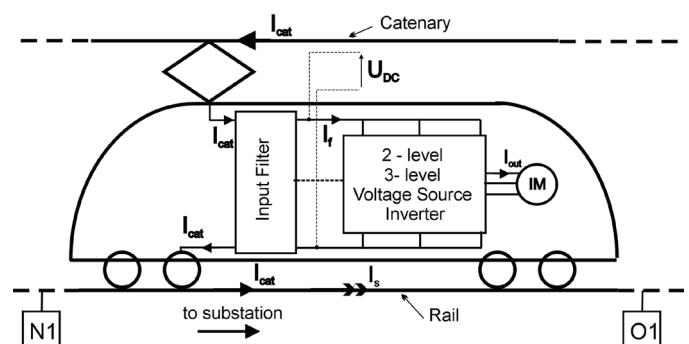


Fig. 1. Scheme of traction vehicle main circuit,  $I_{cat}$  – catenary current,  $I_f$  – DC-link current,  $I_{out}$  – VSI output current

\*e-mail: msteczek@p.lodz.pl

Manuscript submitted 2017-02-28, revised 2017-05-29, initially accepted for publication 2017-06-16, published in October 2017.

Traction drives can operate in a wide range of frequencies and torque. Therefore, the drive must change its control strategy according to the conditions. For example in [9], the author takes under consideration the problem of smooth transition between the PWM technique and square wave (SW) switching strategy for a traction inverter. The proposed schema allows for avoiding torque discontinuity during transition from constant-torque to constant-power operating areas.

## 2. DC side current harmonics limits

In this paper, a comparative study of catenary current spectra generated by 3 kV DC traction vehicles equipped with the two- and three-level inverters was conducted. The results were obtained using a simulation model of a DC-AC 500 kW traction drive verified by means of laboratory measurements carried out for a low-power drive. The results of simulations are related to the limits valid for PKP PLK S.A. railways in Poland [1] (Fig. 2).

Complying to catenary current harmonics limits by traction drives is to ensure the compatibility between rolling stock and the railway signalling system. The reduction of current harmonics generated by VSI-based propulsion systems has been a significant issue since the first vehicles of that kind started to operate. One of the methods for reducing current harmonics generated by VSI drives was proposed in [10], and it is based on re-injection of current harmonics with opposite phase (in comparison to the detected disturbances) into the DC-link. Due to the high operating performance of modern power electronics this technique is feasible, but risky. The detuned reinjection system will provide additional current harmonics into the DC-link. The other group of methods, called the cancellation methods, was proposed for multi-drive vehicles (most of them are high and medium power traction vehicles) [11, 12] and for stationary, grid-connected applications [13]. Applying these techniques

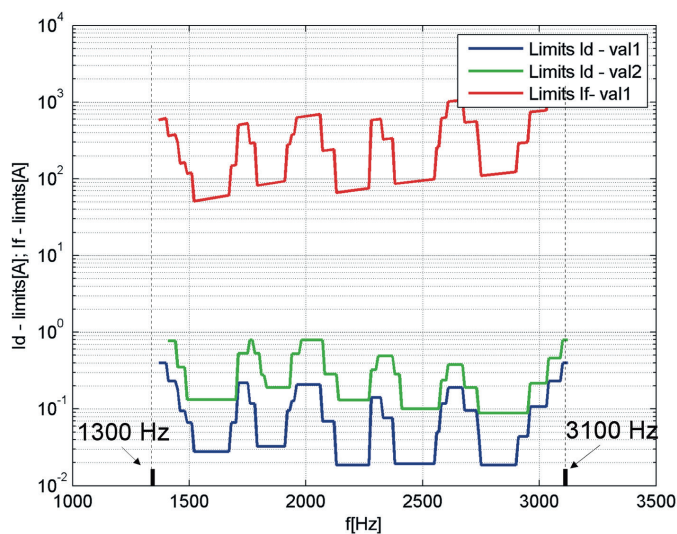


Fig. 2. Limits for catenary ( $I_{cat}$ ) and recalculated for DC-link ( $I_f$ ) current harmonics, generated by a traction vehicle in the frequency band between 1300 and 3100 Hz; val1, val2 – valid limits for Polish railway routes

requires precise parallel cooperation of a minimum two VSIs. One of the main disadvantages of these methods is that their efficiency depends on the balance of drives' loading conditions, which is very difficult to establish in drive conditions.

It seems that the most reliable techniques of controlling the amount of disturbing harmonics in catenary current are the methods based on the development of inverter modulation techniques. It is expected that proper modification of modulation techniques may provide the DC-link current with a significantly reduced level of harmonics amplitudes in the bands of frequencies restricted by compatibility requirements [1].

In this paper, the authors show the impact of a number of voltage levels (two and three) in the VSI on the DC-link ( $I_f$ ) and catenary current ( $I_{cat}$ ) spectra generated by a traction vehicle equipped with an inverter propulsion system. Two limit patterns for current  $I_d$  are specified (Fig. 2): val1 – limits valid for all railway routes in entire Poland and val2 – specified for railway routes, on which devices known to be more susceptible to current disturbances have been decommissioned. The more restrictive limits (val1) will be used as the evaluation criterion in this paper.

The  $I_{cat}$ -limits can be recalculated on the DC-link side of a low pass gamma-type input filter as the 'If-limits'. Assuming that a filter's impedance is linear for higher frequencies, the current  $I_d$  can be recalculated to current  $I_f$ , using impedances of the choke  $Z_{Lf}(j\omega)$  and the capacitor  $Z_{Cf}(j\omega)$  in the equation for impedance current divider:

$$I_f(j\omega) = I_{cat}(j\omega) \cdot \left[ \frac{Z_{Lf}(j\omega)}{Z_{Cf}(j\omega)} + 1 \right] \quad (1)$$

$I_f$  – limits can be compared with the  $I_f$  current harmonics, whose magnitudes are much higher than  $I_{cat}$ , which in turn makes them easy to be detected and measured.

## 3. Traction drive simulation model

The results presented in the remaining part of the paper were obtained by computer simulations carried out for a model of a drive system with two- and three-level VSI respectively supplying a DKLBZ 500 kW induction traction motor used in one of the EMUs operating under 3 kV DC voltage. The applied methodology of modelling was verified by measurements in a low-power drive system laboratory stand (Section 6).

For the present work, the traction drive simulation models (Fig. 3) were implemented using the Matlab Simulink environment. Simulation results were carried out for quasi-steady states of the analysed drive system with usage of time domain transient simulation option. Fig. 4 presents a scheme of one phase of the induction machine model used in simulations. To model the load of traction motor, the fundamental frequency voltage source (SEM) was applied. The power supply for the models was the perfect 3 kV DC voltage  $U_{DC}$  fed from ideal substation without voltage harmonics in output voltage. The parameters of simulation models of laboratory and full-scale traction drives analysed in this paper are presented in Table 1. The

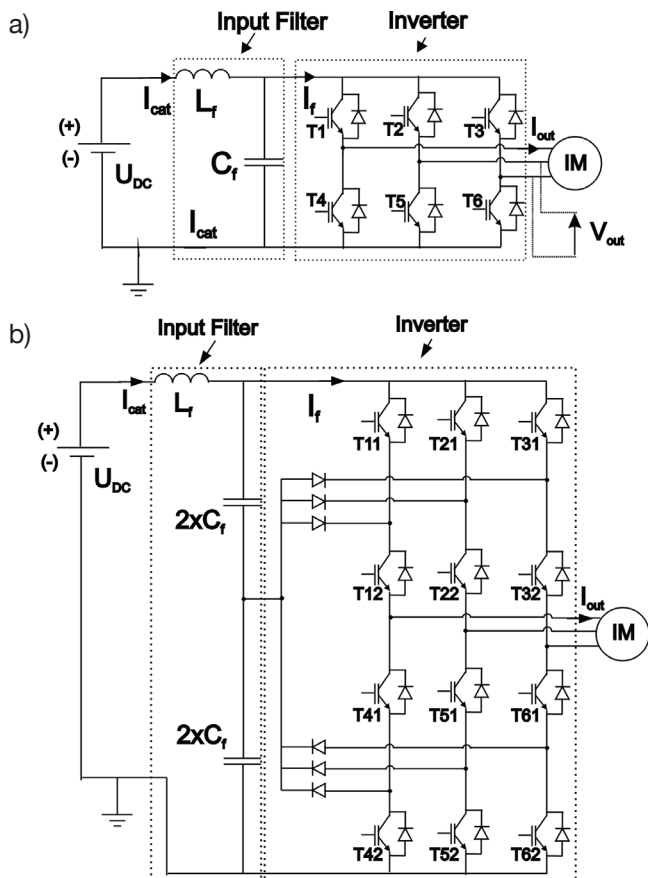


Fig. 3. Schema of the traction VSI: a) 2-level b) 3-level

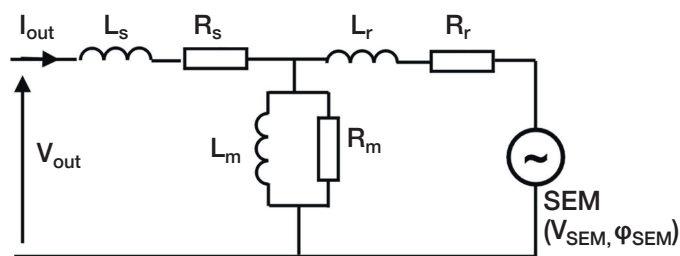


Fig. 4. Simulation model of induction machine (one phase)

Table. 1  
Parameters of induction motor models

| Type                                     | Sf71-2B | DKLBZ   |
|--|---------|---------|
| Rated power – Pn                         | 0.5 kW  | 500 kW  |
| Rated current – In                       | 1.37 A  | 170 A   |
| Rated voltage – Un                       | 380 V   | 1900V   |
| Stator leakage inductance per-phase – Ls | 35.6 mH | 1.56 mH |
| Stator winding resistance per phase – Rs | 14.2 Ω  | 0.107 Ω |
| Rotor leakage inductance per-phase – Lr  | 35.5 mH | 1.6 mH  |
| Rotor resistance per phase – Rr          | 13.2 Ω  | 0.07 Ω  |
| Core loss resistance – Rm                | 1200 Ω  | ∞       |
| Magnetizing inductance – Lm              | 1000 mH | 53 mH   |

harmonic spectrum analysis presented in this paper is based on the post-processed calculations using FFT of voltage and current waveforms determined with a constant time step  $\Delta t = 1 \mu s$ . The assumed time span for FFT was 1s. The influence of inverter snubbers was assumed to be negligible in the analysed frequency band, and it was omitted in the final discussion.

#### 4. SPWM technique

One of the techniques applied for shaping a wave of output voltage of both two- and three-level inverters is SPWM. In this modulation technique, the gate signals for the inverter's transistors are generated by comparison of the sinusoidal reference signal ( $U_{ref}$ ) with one or more carrier waveforms ( $U_{car}, U_{car1}, U_{car2}$ ). Exemplary control signals for the two-level VSI are shown in Fig. 5a ( $UT1$ ), while for the three-level VSI – in Fig. 5b ( $UT11, UT12$ ). In the three-level VSI, the control signal is divided into two transistors for each leg of the inverter (Fig. 3b, T11-T12 and complementary T41-T42).

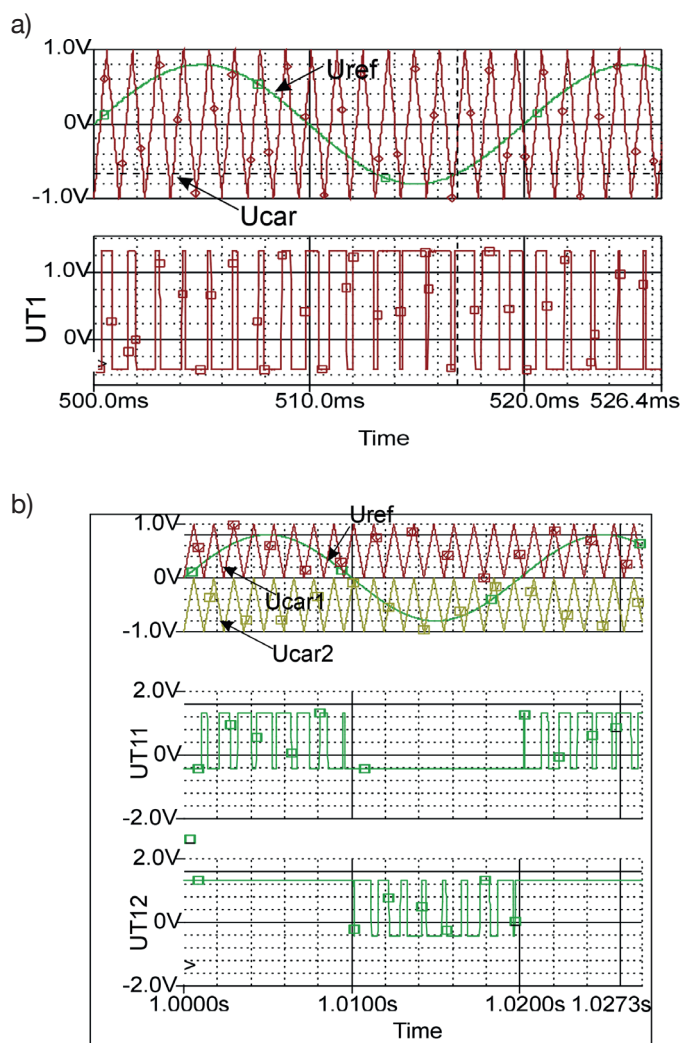


Fig. 5. Control signals for two (a) and three (b) level inverters,  $U_{ref}$  – reference signal,  $U_{car}$  – carrier signal,  $UT$  – transistor gate signal

SPWM modulation is easy to apply due to the lack of requirements to store a great amount of data in a microcontroller's memory. However, it does not provide an opportunity to influence the required specific harmonics of the generated output voltage.

### 5. SHE modulation

The SHE modulation is one of the non-carrier based techniques. It was described for the first time in 1960s [14] and it was developed by Patel and Hoft in [15, 16]. Control of the VSI transistors with the use of this technique is based on direct determination of switching angles (time points) and sending control signals to the transistor gates, according to these points.

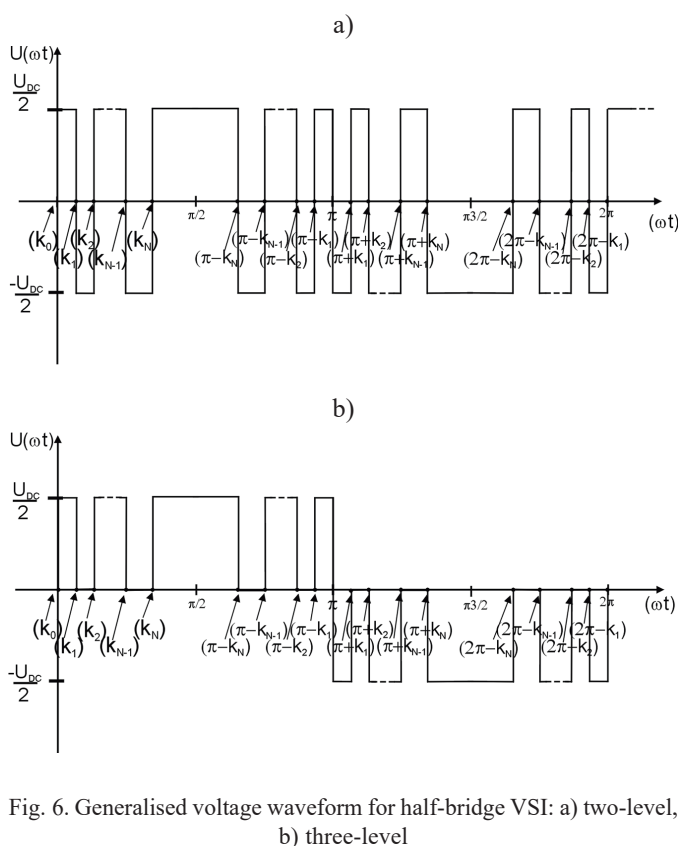


Fig. 6. Generalised voltage waveform for half-bridge VSI: a) two-level, b) three-level

The switching angles are calculated from a set of non-linear equations formulated by a Fourier series for generalised voltage waveforms defined for the two- and three-level VSI, respectively (Fig. 6). Formulation of the equation set is based on the Euler's coefficients for  $a_0$ ,  $a_n$ ,  $b_n$  calculations as in (7) and (9).

$$f(\omega t) = a_0 + \sum_{n=1}^{\infty} [a_n \sin(n\omega t) + b_n \cos(n\omega t)] \quad (2)$$

where:  $a_0$ ,  $a_n$  and  $b_n$  – coefficients described by Euler's formulas.

Assuming quarter-wave symmetry the function has to fulfil the following two conditions:

$$f(\omega t) = -f(\omega t + \pi) \quad (3)$$

$$f(\omega t) = f(\pi - \omega t). \quad (4)$$

For this type of symmetry, the coefficients  $a_0$  and  $b_n$  are equal to zero. For the two-level waveform (Fig. 6a) the coefficient  $a_n$  can be written as:

$$a_n = \frac{1}{\pi} \int_0^{2\pi} f(\omega t) \sin(n\omega t) d(\omega t). \quad (5)$$

For the two-level:

$$a_n = \frac{1}{\pi} \left[ \int_0^{k_1} \frac{U_{DC}}{2} \sin(n\theta) d(\theta) + \int_{k_1}^{k_2} -\frac{U_{DC}}{2} \sin(n\theta) d(\theta) + \dots + \int_{2\pi - k_2}^{2\pi - k_1} \frac{U_{DC}}{2} \sin(n\theta) d(\theta) + \int_{2\pi - k_1}^{2\pi} -\frac{U_{DC}}{2} \sin(n\theta) d(\theta) \right]. \quad (6)$$

Therefore, for odd and even  $n$  it can be given by:

$$a_n = \begin{cases} \frac{4 \cdot U_{DC}}{2n\pi} \left[ 1 + \sum_{i=1}^N (-1)^i \cdot 2 \cos(n \cdot k_i) \right] & \text{for odd } n \\ 0 & \text{for even } n \end{cases} \quad (7)$$

For the three-level (Fig. 6b), the coefficient  $a_n$  can be described as follows:

$$a_n = \frac{1}{\pi} \left[ \int_0^{k_1} \frac{U_{DC}}{2} \sin(n\theta) d(\theta) + \int_{k_2}^{k_3} \frac{U_{DC}}{2} \sin(n\theta) d(\theta) + \dots - \int_{2\pi - k_2}^{2\pi - k_3} \frac{U_{DC}}{2} \sin(n\theta) d(\theta) - \int_{2\pi - k_1}^{2\pi} \frac{U_{DC}}{2} \sin(n\theta) d(\theta) \right]. \quad (8)$$

Therefore, for odd and even  $n$  it can be given by:

$$a_n = \begin{cases} \frac{2 \cdot U_{DC}}{2n\pi} \left[ 1 + \sum_{i=1}^N (-1)^i \cdot \cos(n \cdot k_i) \right] & \text{for odd } n \\ 0 & \text{for even } n \end{cases} \quad (9)$$

The number of equations in the system describing the SHE problem is equal to the number of switching angles in the quarter-period  $N$ . Regarding this,  $N-1$  voltage harmonics can be eliminated from the inverter's output voltage and the fundamental component can be fixed. The above equations will be used to calculate the switching angles for the VSI models in

order to analyse the differences between the catenary current spectra generated by two and three-level traction drive systems with the SHE modulation technique.

The SHE technique provides the opportunity not only to eliminate the chosen voltage harmonics, but also to control their values. This technique can be used to directly shape the spectra of uncontrolled voltage harmonics [17] and, following indirectly, the spectra of DC-link current harmonics [18].

## 6. Verification of the simulation model

In order to assess the accuracy of the simulation model of the traction drive system – applied in the further part of the study for calculation of harmonics spectra – a set of laboratory measurements in a low-power drive system laboratory stand (Fig. 7) was developed.

This stand is composed of a two-level SHE controlled VSI, supplying a 500 W induction motor. A dSpace1104 card has been applied, which allowed for use of off-line calculated switching angles (SHE method) stored in a look-up table.

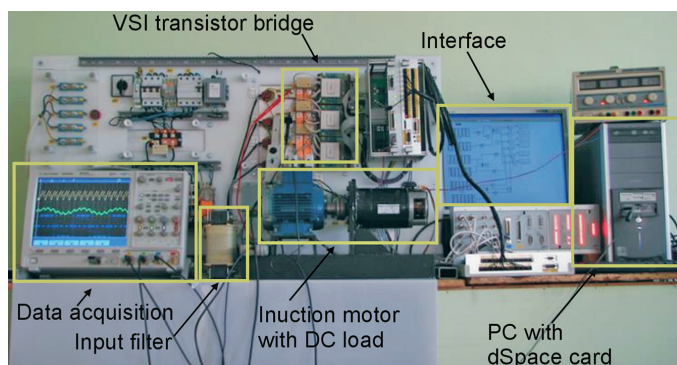


Fig. 7. Picture of laboratory stand

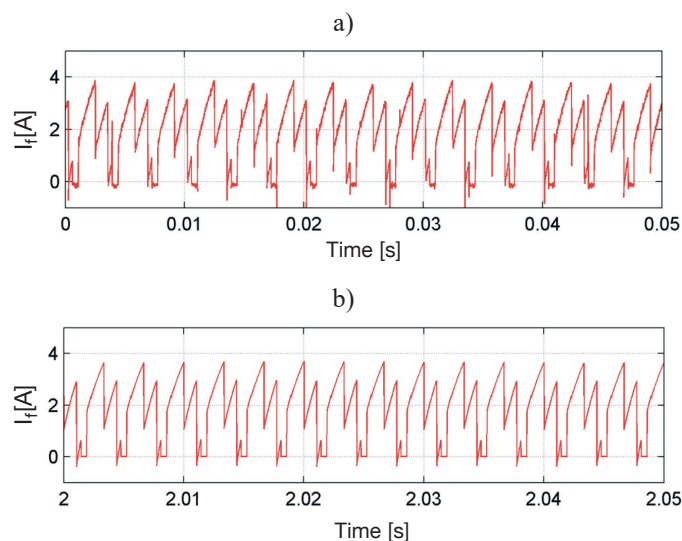


Fig. 8. Waveform of a DC-link current  $I_f$  for SHE modulation ( $M_5 = 0.1$ ): a) measurements b) simulation

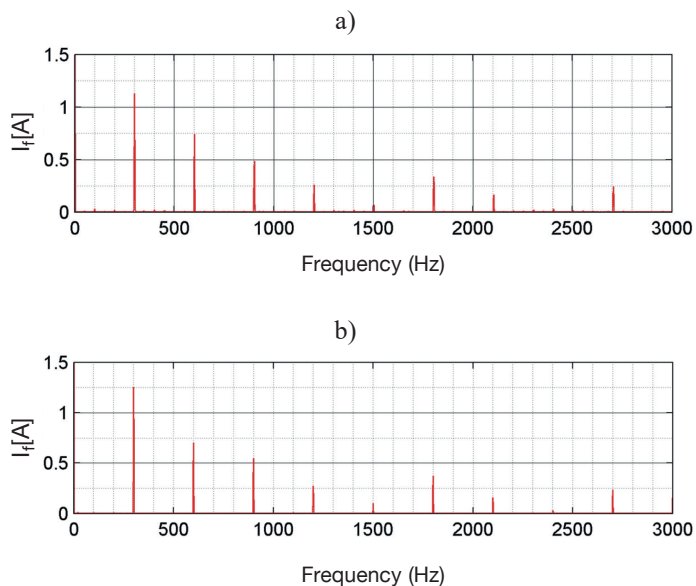


Fig. 9. Harmonics spectra of a DC-link current  $I_f$  shown in Fig. 7 for SHE modulation ( $M_5 = 0.1$ ): a) measurements b) simulation

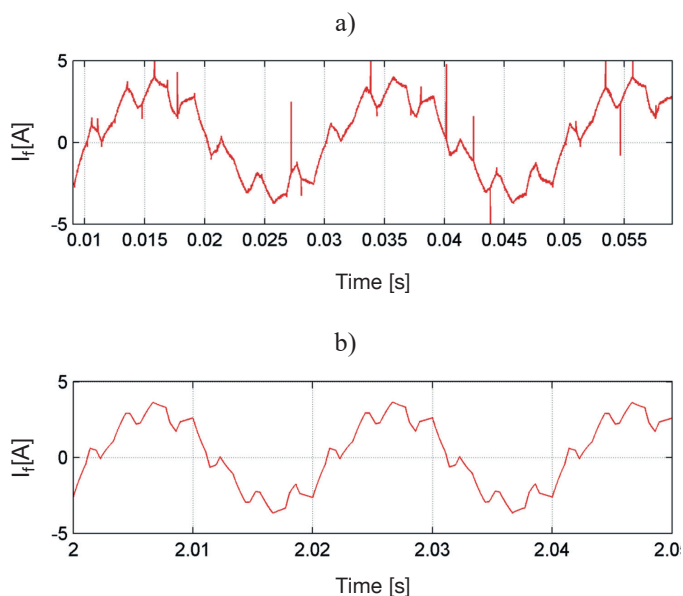


Fig. 10. Waveform of the motor's phase current  $I_{out}$  SHE modulation ( $M_5 = 0.1$ ): a) measurements b) simulation

A DC generator was used as load of the motor during measurements in its steady-state operating points.

The accuracy assessment of the assumed simulation model of the drive was performed using the following results: waveforms (Fig. 8) and harmonics spectra (Fig. 9) of DC-link current  $I_f$ ; waveforms (Fig. 10) and harmonics spectra (Fig. 11) of a motor's phase current  $I_{out}$ . The graphs present the comparison of exemplary results of simulations and measurements for one operating point designated by parameters:  $M_1 = 0.65$  and  $f_{fal} = 50$  Hz.

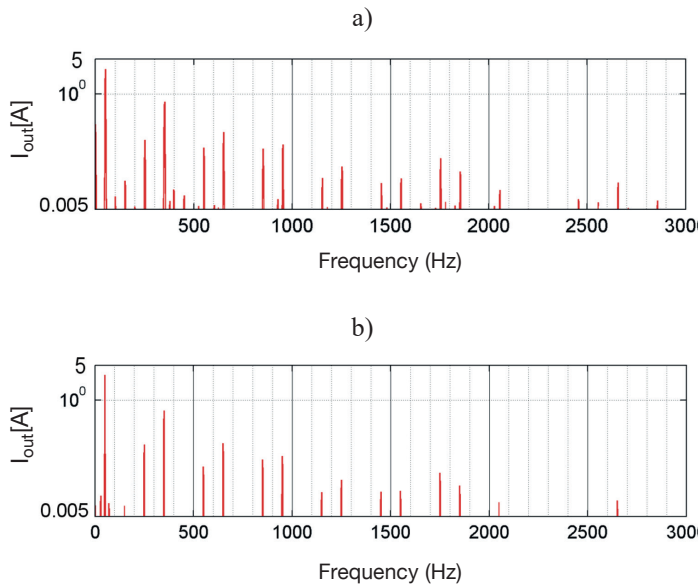


Fig. 11. Harmonics spectra of the motor's phase current  $I_{out}$  shown in Fig. 9, for SHE modulation ( $M_5 = 0.1$ ): a) measurements b) simulation

The comparative analysis of the results obtained by simulation and measurements in a laboratory low-scale setup allows for stating that the derived simulation model of a VSI drive with PWM control is accurate enough to be used for analysis of harmonics spectra in a traction drive system.

### 7. Influence of non-balanced neutral point voltage in 3-level VSI

Before the comparison between the spectra of the two-level and the three-level high power VSI can be delivered, it is essential to analyse the influence of lack of neutral point voltage balancing in the three-level NPC VSI. The techniques of neutral point voltage balancing in multilevel inverters are described in literature for both PWM [8] and SHE [7] modulations. How-

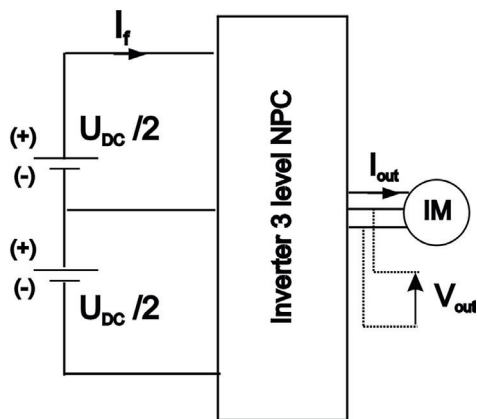


Fig. 12. VSI simulation model schema without an input filter circuit

ever, this article does not present balancing techniques due to the fact that their influence on generated harmonics is outside of the scope of this paper.

To prove that the voltage balancing problem has no impact on the results presented in the article, the simulation results acquired by means of a model with an input filter (Fig. 3b) were compared with the results acquired by means of a model without an input filter (Fig. 12). Replacing filter capacitors with two identical voltage sources excludes the effect of neutral point voltage fluctuations in the multilevel VSI. Figures 13 and 14 show that the voltage balancing problem has no influence on  $I_f$  current spectrum in the analysed frequency band between 1300 and 3100 Hz.

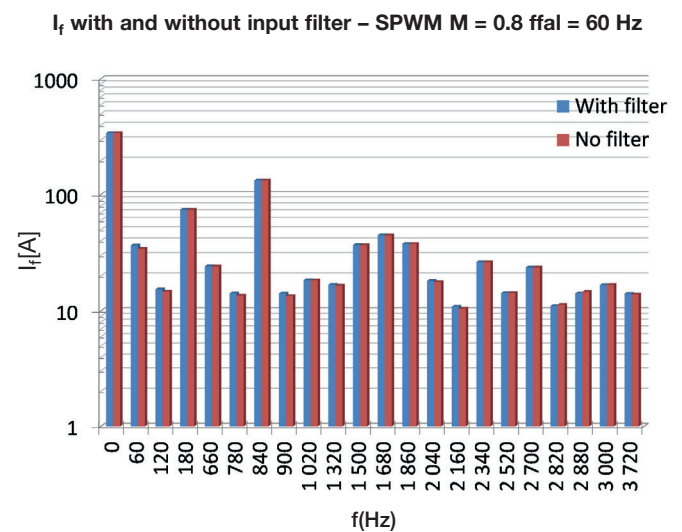


Fig. 13. Comparison between the spectrum  $I_f$  with and without influence of the neutral point voltage unbalancing for SPWM modulation

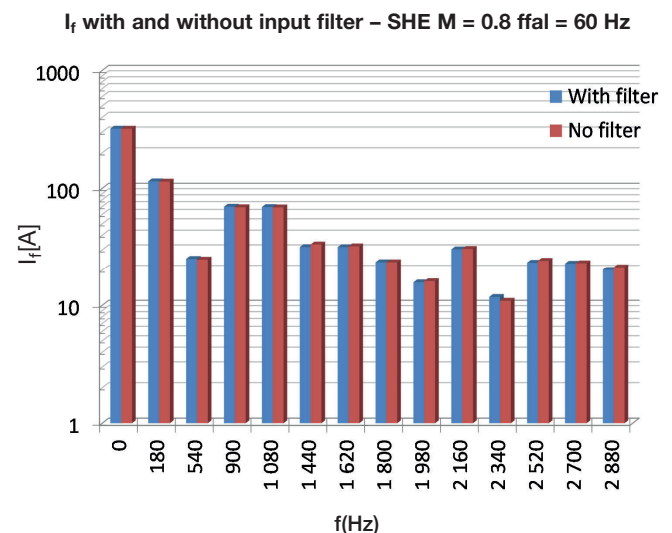


Fig. 14. Comparison between the spectrum  $I_f$  with and without influence of the neutral point voltage unbalancing for SHE modulation

## 8. Comparison between current spectra – SPWM modulation – 3 kV simulation model

This Section presents a comparative analysis of the spectra harmonics of DC-link  $I_f$  and catenary  $I_{cat}$  currents, respectively, generated by the two- and three-level VSI with SPWM control technique in a drive system of a traction vehicle. The results were obtained by simulation of a six steady-state operating points of the 500 kW model of the VSI with SPWM modulation for a carrier frequency  $f_c = 840$  Hz and sinusoidal reference waveform  $f_{fal} = 20 \div 70$  Hz. The topology of the compared VSI is presented in Fig. 3. Assuming that the harmonics generated by each of the VSI on-board of a traction vehicle sum up at an input point of common coupling (the worst case), the amplitude limits of harmonics for each of the VSI input DC current harmonics were proportionally reduced to  $1/4$  of the limit for the whole 4-VSI EMU and to  $1/8$  for a train composed of two such EMUs. Limits for DC-link current  $I_f$  were rescaled individually for each inverter due to attenuation of the LC input filter with parameters  $L_f = 8.7$  mH,  $C_f = 6.5$  mF.

**8.1. Two-level VSI current spectrum.** For comparison purposes, spectra of current harmonics  $I_{cat}$  and  $I_f$  generated by the two-level inverter are shown in Fig. 15. All harmonics of current  $I_f$  are observed in current  $I_{cat}$ .

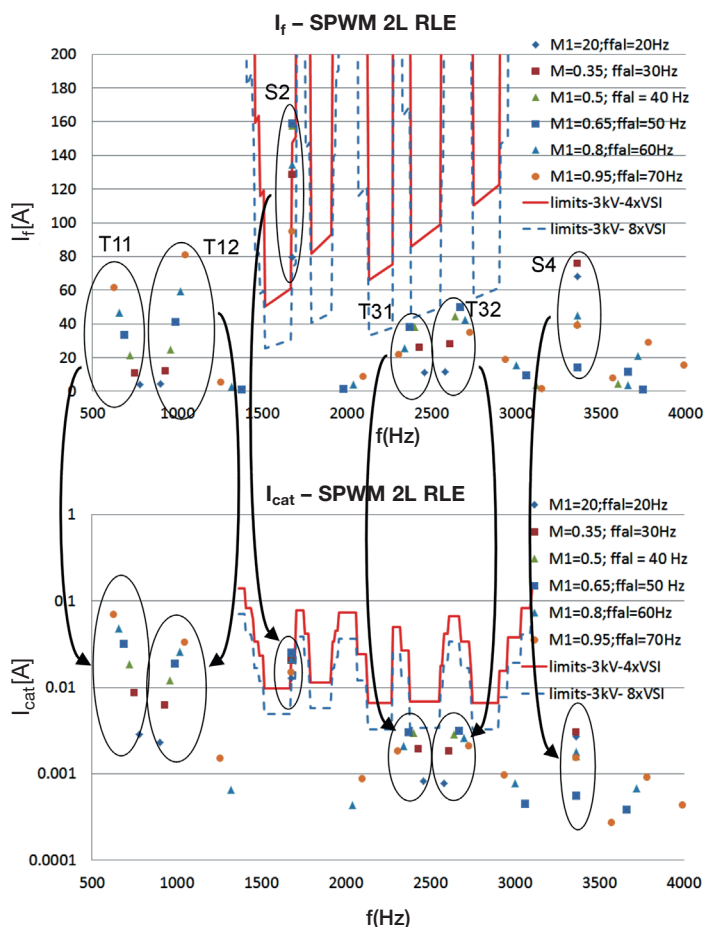


Fig. 15. Spectra of harmonics currents  $I_f$  and  $I_{cat}$  for the two-level VSI

The spectra of harmonics of currents  $I_f$  and  $I_{cat}$  generated by the two-level VSI can be divided into stationary harmonics assigned as ‘S’, and travelling harmonics signed as ‘T’. The frequency of the harmonics ‘S’ is dependent only on the carrier frequency ( $f_c$ ), while the frequency of harmonics ‘T’ on the difference between the  $f_c$  and  $f_{fal}$ . Their frequencies can be described as follows:

$$\text{stationary 'S': } f_{f_s} = p \cdot f_c \quad \forall \text{ even } p \quad (10)$$

$$\text{travelling 'T': } f_{f_t} = p \cdot f_c \pm 3 \cdot f_{fal} \quad \forall \text{ odd } p. \quad (11)$$

In Fig. 15, it may be observed that a stationary harmonic signed as ‘S2’ is to be found both in  $I_f(f)$  as well as in  $I_{cat}(f)$  spectra, and its amplitude in  $I_{cat}(f)$  exceeds the assumed limit.

**8.2. Three-level VSI current spectrum.** Figure 16 presents spectra of the harmonics of currents  $I_{cat}$  and  $I_f$  generated by the three-level VSI. It is worth underlining that not all harmonics seen in the current  $I_f$  are observed in the current  $I_{cat}$ .

The spectra of harmonics of currents  $I_f$  and  $I_{cat}$  generated by a three-level NPC inverter can be divided, similarly as for the two-level inverter, into stationary harmonics denoted as ‘S’ and travelling harmonics denoted as ‘T’. Their frequencies can be described as follows:

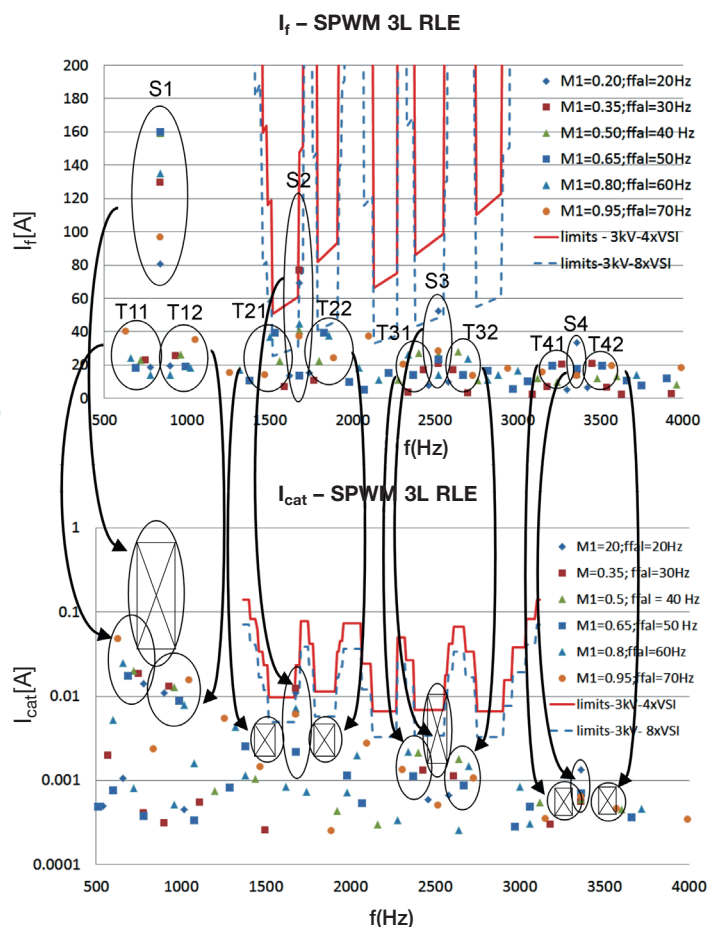


Fig. 16. Spectra of harmonics currents  $I_f$  and  $I_{cat}$  for three-level VSI

stationary ‘S’:  $f_{I_{f_s}} = p \cdot f_c \quad \forall p = 1, 2, 3 \dots$  (12)

travelling ‘T’:  $f_{I_{f_t}} = p \cdot f_c \pm 3 \cdot f_{fal} \quad \forall p = 1, 2, 3 \dots$  (13)

The frequencies of  $I_{cat}$  current harmonics are identical as for the two-level inverter and can be described by formulas (10, 11).

In the case shown in Fig. 16, the amplitudes ‘S2’ and ‘S3’ of two harmonics are above the assumed limits, while there is no harmonic ‘S3’ in the spectrum of current  $I_{cat}$ . Therefore, it may be stated that an application of the three-level inverter with SPWM control has not eliminated the amplitude of harmonic ‘S2’ in the catenary current  $I_{cat}$ .

**8.3. Comparison between the two-level and three-level VSI current spectrum.** Figures 17 and 18 show a comparison of spectra of the two and three-level VSI waveforms:  $I_{cat}$  and  $I_f$  for

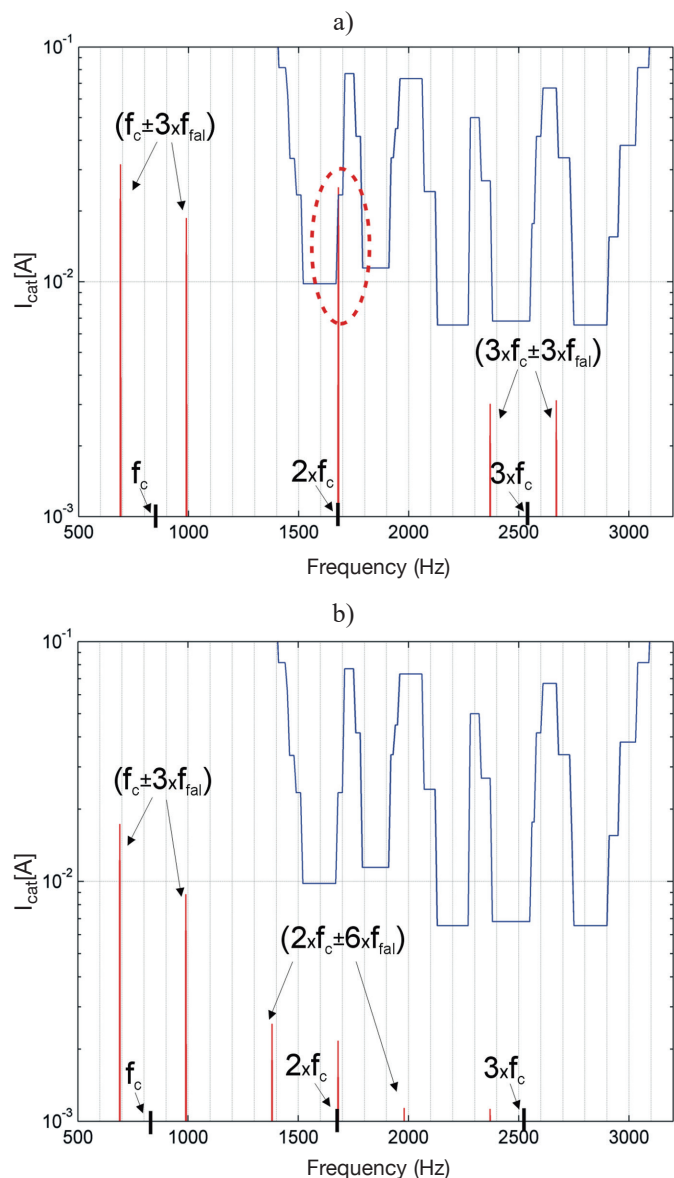


Fig. 17. Harmonic spectrum of current  $I_{cat}$  for the SPWM modulation a) two-level b) three-level VSI

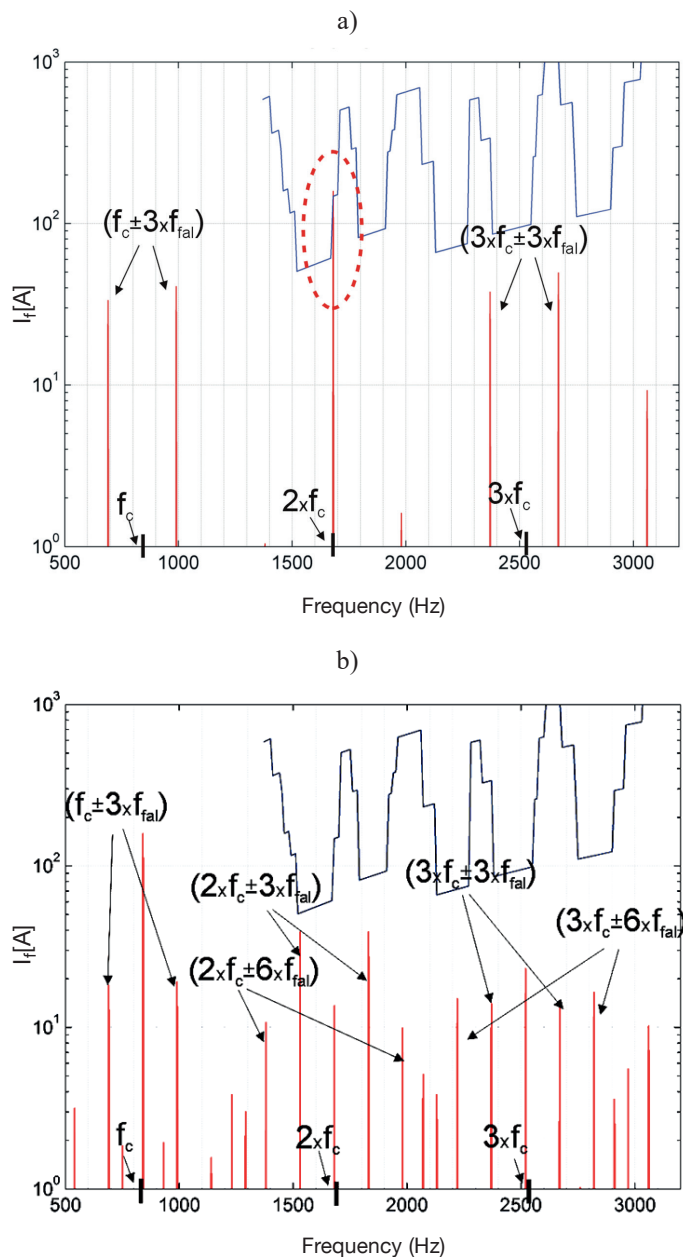


Fig. 18. Harmonic spectrum of current  $I_f$  - SPWM modulation a) two-level b) three-level VSI

one operating point:  $f_{fal} = 50$  Hz,  $M1 = 0.65$ ,  $f_c = 840$  Hz. The presented exemplary results allow for observing the disturbing influence of a current harmonic with frequency ( $2x f_c$ ) generated in the two-level VSI drive.

In Fig. 16b, it is seen that at the analysed operating point of the three-level VSI this harmonic amplitude does not exceed the limit; however, we cannot project this effect to the whole range of operation which may be seen in Fig. 15 (harmonic ‘S2’). It may be concluded that by changing only the two-level VSI into the three-level on board of a traction vehicle (in this case EMU) without changing the technique of modulation, it is not possible to guarantee the compatibility of a traction vehicle with signalling and control systems installed on a railway line.

### 9. Comparison between current spectra – SHE modulation – 3 kV simulation model

The comparison between two and three-level VSIs with the SHE modulation was provided with assumption that the lower orders of voltage harmonics are eliminated. The number of switching angles  $N$  in a quarter-period was fixed in such a manner so as to establish transistor switching frequency similar to the switching frequency used for the SPWM analysis. The modulation index ( $M1$ ), fundamental frequency ( $f_{fal}$ ), number of switching angles in quarter-period ( $N$ ) and orders of the eliminated harmonics for selected harmonics are presented in Table 2.

Table 2  
Parameters of VSI operating points

| M1   | $f_{fal}$ [Hz] | N  | Eliminated harmonics   |
|------|----------------|----|--|
| 0.2  | 20             | 17 | 5, 7, 11, 13, 17, 18, 23, 25, 29, 31, 35, 37, 41, 43, 47, 49 |
| 0.35 | 30             | 12 | 5, 7, 11, 13, 17, 18, 23, 25, 29, 31, 35                     |
| 0.5  | 40             | 8  | 5, 7, 11, 13, 17, 18, 23                                     |
| 0.65 | 50             | 6  | 5, 7, 11, 13, 17   |
| 0.8  | 60             | 5  | 5, 7, 11, 13   |
| 0.95 | 70             | 4  | 5, 7, 11   |

Implementation of the SHE modulation allowed for successful elimination (according to the assumptions) of low-order harmonics in voltage  $V_{out}$  (Fig. 19). It can also be observed that when the three-level VSI is applied, the non-controlled harmonics have lower amplitudes (below the ‘envelope’ in Fig. 19b, compared with a). Therefore, amplitudes of the current  $I_{cat}$  harmonics were lower as well.

Replacing the two-level VSI with the three-level on-board of the 2 MW EMU with four driven axles with individual VSI allows for fulfilling the limits of input current harmonics not only for a single EMU, as in the case with two-level VSI (Fig. 20a), but even for a double EMU set in a train of a total power of 4 MW (Fig. 20b).

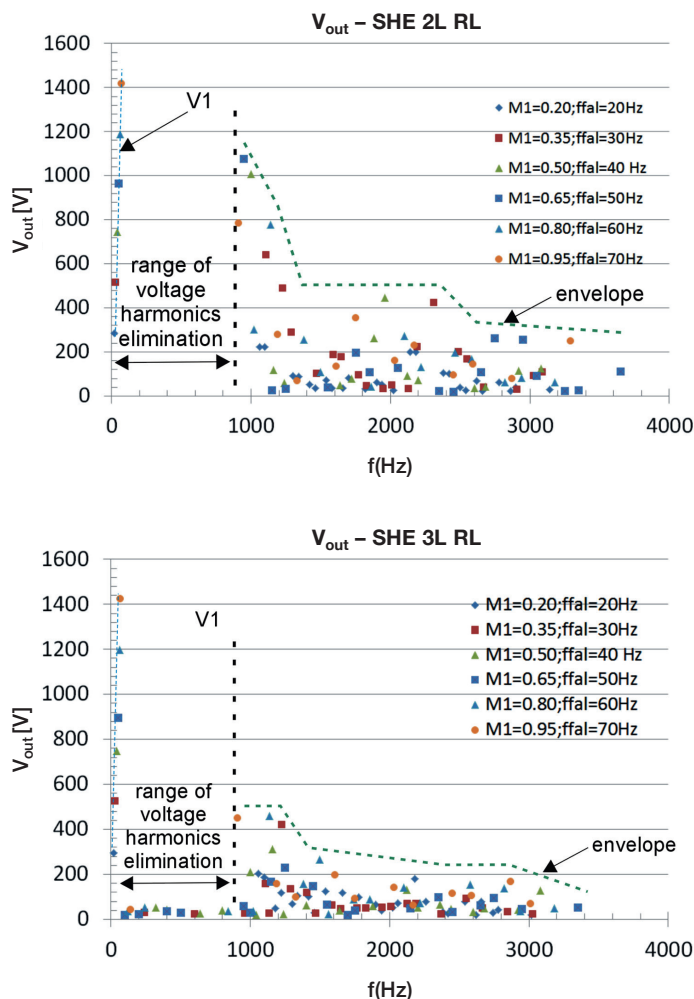


Fig. 19. Harmonic spectrum of voltage  $V_{out}$ : a) 2-level b) 3-level VSI

The SHE modulation is non-carrier based type, and that is why there are no stationary harmonics. All generated harmonics depend only on the frequency of the fundamental component  $f_{fal}$ . Assuming that the generated voltage waveform  $V_{out}(t)$  fulfils condition of half- (3) and quarter-wave (4) symmetry, the

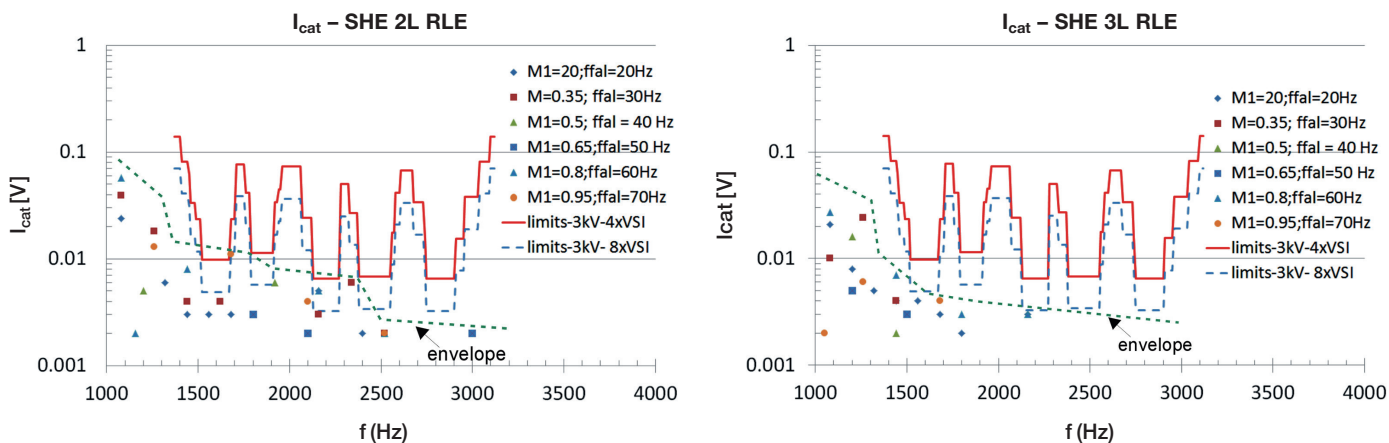


Fig. 20. Harmonic spectrum of current  $I_{cat}$ : a) 2-level b) 3-level VSI

following harmonics will occur in the spectra  $V_{out}(f)$  for both, the two- and three-level inverters:

$$f_{Vout} = (p \cdot 6 \pm 1)f_{fal} \quad \forall \quad p = 1, 2, 3 \dots \quad (14)$$

The modulation of this kind generates the same orders of catenary current harmonics  $I_{cat}(f)$  for both solutions:

$$f_{Icat} = p \cdot 6 \cdot f_{fal} \quad \forall \quad p = 1, 2, 3 \dots \quad (15)$$

In the two-level VSI drive, all harmonics  $I_f$  are visible in spectrum  $I_{cat}$  (Fig. 21a). In DC-link of the three-level VSI drive additional harmonics occurs. The additional harmonics orders are triple odd multiplication of the VSI fundamental frequency.

Order of the harmonics  $I_f$  for the three-level (Fig. 21b) can be described as follows:

$$\begin{cases} f_{I_f} = p \cdot 6 \cdot f_{fal} & \forall \quad p = 1, 2, 3 \dots \\ f_{I_f} = p \cdot 3 \cdot f_{fal} & \forall \quad \text{odd } p \end{cases} \quad (16)$$

See that limits in Fig. 21a are significantly lower than limits in Fig. 21b due to attenuation effect of an input filter. Monitoring of the disturbances generated by the traction vehicle equipped with the three-level inverter can be provided by measuring DC-link current, with odd triple harmonics being ignored. For this purpose a measurement system should be delivered with parameters of the drive's operating point (fundamental frequency).

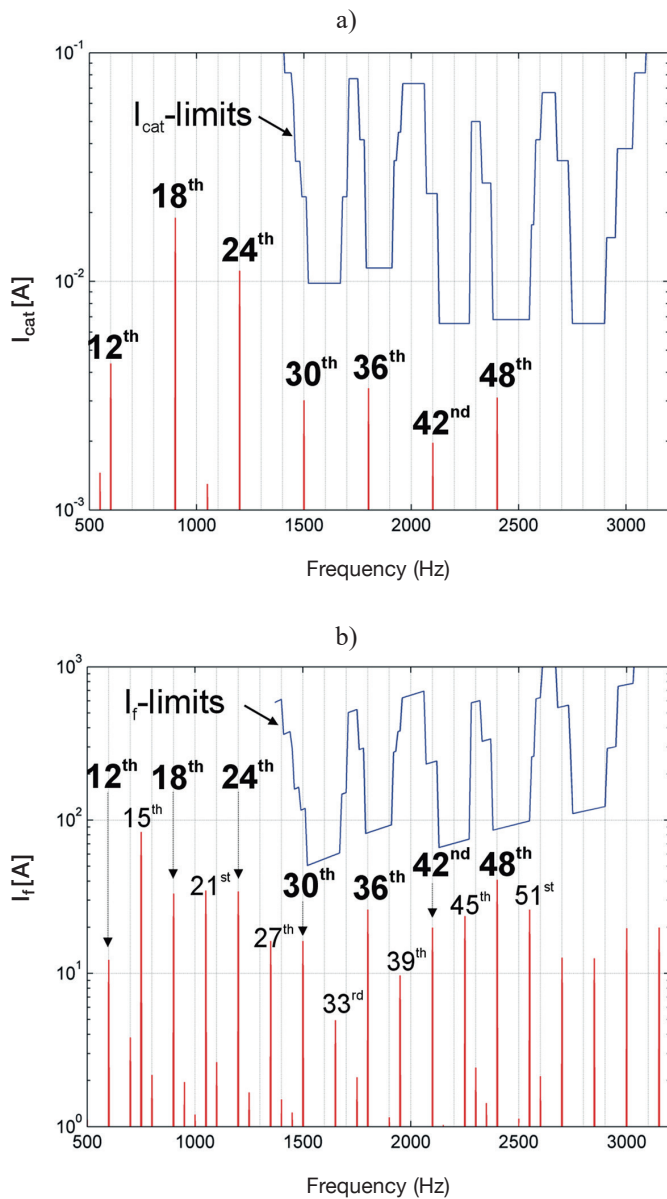


Fig. 21. Simulation results of the current spectrum generated by the three-level VSI based traction drive with applied SHE modulation  
a)  $I_{cat}$  – catenary current b)  $I_f$  – DC-link current

## 10. SHE – optimization of the solution

The SHE problem is a non-linear one. Thus, multiple solutions of switching angles may exist. One of the methods to find the most suitable solution may be to search within the area of possible solutions with assumed restrictions (generating as many solutions as possible for a defined point of operation of the VSI – operation frequency  $f_{fal}$  and an amplitude of the fundamental voltage harmonic  $V_{out}$ ) and choosing the best ones according to the assumed criteria. For instance, in [19] THDI minimization has been selected as a criterion. In [20], dual criterion has been taken into account: elimination of some harmonics and minimization of another group of harmonics. Typically, the Newton-Rapson method of solving non-linear equations has been applied. In [21], solving of non-linear equations has been brought to an optimization problem with application of particle swarm optimization (PSO), which significantly improved efficiency of the process of finding a solution.

The problem of the compatibility of the VSI equipped traction vehicles with the railway signalling and control system, which is analysed in this paper, is associated with maintaining specific input current harmonics amplitudes below the set limits. Therefore, the harmonics of DC side current have been assumed as basic criteria. The similar approach is presented in [22], but a combination of SHE and SHM (selective harmonic mitigation) techniques was used to solve the problem. In present work, in order to get as many solutions of SHE control as possible, and then compare them with the criterion, it is required to obtain multiple solutions of the set of non-linear equations (7, 9), each time with different starting points.

In order to create a vector of random starting points  $x_0$  composed of starting values  $\alpha_0$ , a vector of intervals  $x_{0int}$  was created, in which specific starting points were drawn for further calculations. An illustration of a drawn schema of starting points was presented in Fig. 22.

$$\mathbf{x}_0 = [\alpha_0 \alpha_1 \alpha_2 \alpha_3 \dots \alpha_{N-1} \alpha_N] \quad (17)$$

$$\mathbf{x}_{0int} = [int_0 \ int_1 \ int_2 \ \dots \ int_{N-1} \ int_N] \quad (18)$$

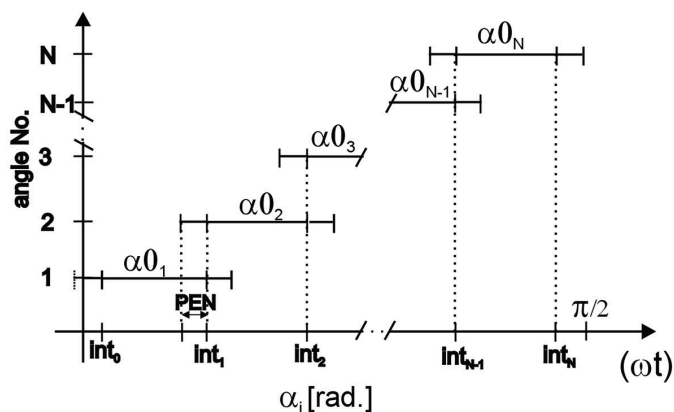


Fig. 22. Illustration of drawing schema of starting points in fixed bounds

$$\begin{cases} \alpha 0_i = \text{int}_{i-1} + PRV \cdot (\text{int}_i - \text{int}_{i-1}) + \\ \quad + PEN \cdot (-1)^{\text{round}(2 \cdot PRV)} \\ \text{where: } PRV - \text{pseudo random value} \in \langle 0, 1 \rangle \\ \quad PEN - \text{penetration factor} \end{cases} \quad (19)$$

To illustrate the influence of the selected solution on the current  $I_{cat}$  spectra, a simulation analysis for the 500 kW three-level drive system was conducted. Two SHE solutions ('SOL1', 'SOL2') for one operating point of the inverter ( $M1 = 0.7$ ,  $f_{fal} = 50$  Hz,  $N = 5$ ) were calculated. Fig. 23 presents a comparison between the  $I_{cat}$  spectra for both solutions with limits recalculated for 4 and 8 drives operating in parallel in one EMU.

It can be observed that changing the SHE solution from 'SOL1' into 'SOL2' maintains the same operating point ( $M1, f_{fal}$  - unchanged), but the 'SOL2' fulfils limits recalculated even

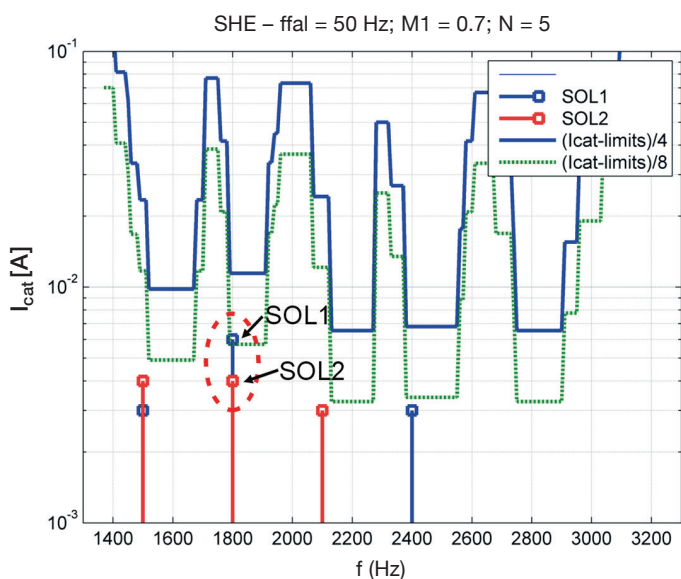


Fig. 23. Spectra of the current  $I_{cat}$  for SHE solutions 'SOL1' and 'SOL2',  $(I_{cat-limits})/4$  – limits decreased for 4 drive EMU,  $(I_{cat-limits})/8$  – limits decreased for 8 drive EMU

for the 8-drive EMU, which makes it more suitable for implementation.

SOL1 –  $x = [0.2805 \ 0.5138 \ 0.9915 \ 1.2141 \ 1.4081]$   
 SOL2 –  $x = [0.1529 \ 0.2573 \ 1.0864 \ 1.3521 \ 1.3893]$

## 11. Conclusions

The paper discusses the problem of compatibility between the modern electric traction vehicles equipped with VSI drives supplied by 3 kV DC voltage and signalling, command and control in railway systems. The two and three-level VSI with different control methods: SPWM and SHE were analysed and compared with application of a simulation model of the 500 kW drive. The accuracy of the derived model was verified by measurements in a low-scale drive system laboratory stand. The analysis of harmonics in DC side input current of the vehicle was undertaken for a range of frequencies restricted by the regulations of the Polish State Railway.

The results of simulations were discussed, and it may be concluded that applying three-level VSI with SPWM control instead of the two-level type on-board of a traction vehicle without the proper choice of control method may not guarantee solving compatibility problems in the analysed frequency bands: 1.3–3.1 kHz. The application of SHE method allowed for fulfilling restrictive railway criteria in the analysed case, even for two combined EMUs composed of eight 500 kW drives. In order to improve process of finding solutions of switching angles in the SHE method according to the defined criteria, the application of an optimized approach to the classical SHE was proposed.

Using the SHE modulation technique, every operating point of the drive requires solving a set of non-linear equations, which implies higher computational effort than the regular sinusoidal PWM. Due to this fact, the off-line method is proposed for solving SHE equations to calculate the switching angles, which are stored in the processor memory as a function of modulation index in the form of a look-up table. Stored switching angles can be retrieved from the processor memory for any operating point during real time application. This solution does not require high processing power of the microcontroller and it is suitable for implementation in the conventional traction inverters. This approach provides control over a drive system in real-time with no need to use very expensive microcontrollers, which perform real-time calculations of the switching angles.

**Acknowledgements.** The authors would like to express their appreciation to Piotr Chudzik, Ph.D., Eng., from Lodz University of Technology for the help during laboratory measurements and all valuable suggestions.

## REFERENCES

- [1] A. Białoń, A. Kazimierzczak, J. Furman, Ł. Zawadka, D. Adamski, P. Pajka, and K. Ortel, "Defining limits and levels of disturbances in signalling and control railway systems", Railway Institute, Warsaw, Report 4430/10 for PKP PLK S.A. (in Polish), 2011.

- [2] H. Bernhard, A. Mariscotti, and D. Wuergler, "Recommendations for the calculation of the total disturbing return current from electric traction vehicles", *IEEE Transactions on Power Delivery* 19 (3), 1190–1197 (2004).
- [3] A. Ogunsola and A. Mariscotti, "Electromagnetic compatibility in railway. Analysis and management", *Lecture Notes in Electrical Engineering*, Springer-Verlag Berlin, 1–528 (2013).
- [4] A. Choudchury, P. Pillay, and S.S. Williamson, "Comparative analysis between two-level and three-level DCAC electric vehicle traction inverters using a novel DC-link voltage balancing algorithm", *IEEE Journal of Emerging and Selected Topics in Power Electronics* 2 (3), (2014).
- [5] D. Prajapati, V. Ravindran, J. Sutaria, and P. Patel, "A comparative study of three phase 2-level VSI with 3-level and 5-level diode clamped multilevel inverter", *International Journal of Emerging Technology and Advanced Engineering* 4 (4), 708–713 (2014).
- [6] R.K. Behera, S.P. Das, and O. Ojo, "Utility friendly three-level neutral point clamped converter-fed high-performance induction motor drive", *IET Power Electron.* 5 (7), 1196–1203 (2012).
- [7] S.R. Pulikanti, M.S.A. Dahidah, and V.G. Adelidis, "Voltage balancing control of three-level active NPC converter using SHE-PWM", *IEEE Trans. on Power Delivery* 26 (1), (2011).
- [8] A. Choudchury, P. Pillay, S.S. Williamson, "A hybrid PWM based DC-link voltage balancing algorithm for a three-level NPC DC/AC traction inverter drive", *IEEE Journal of Emerging and Selected Topics in Power Electronics* 3 (3), (2015).
- [9] A. Ghaderi, T. Umeno, and M. Sugai, "An altered PWM scheme for single-mode seamless control of AC traction motors for electric drive vehicles", *IEEE Trans. on Ind. Electron.* 63 (3), (2016).
- [10] C. Broche, J. Lobry, P. Colignon, and A. Labart, "Harmonic reduction in DC link current of a PWM induction motor drive by active filtering", *IEEE Trans. Power Electron.* 7 (4), (1992).
- [11] H. Ye and A. Emadi, "An interleaving scheme to reduce DC link current harmonics of dual traction inverters in hybrid electric vehicles", *IEEE A Power Electron. Conf. and Exp.*, 3205–3211 (2014).
- [12] T. Ogawa and S. Wako, "Theoretical analysis of cancellation of DC-link current harmonics in the inverter-controlled DC electric railcar", *IEEE European Conf. on Power Electron.*, 1–10 (2007).
- [13] Y. Yang, P. Davari, F. Zare, and F. Blaabjerg, "A DC-link modulation scheme with phase-shifted current control for harmonic cancellations in multidrive applications", *IEEE Trans. Power Electron.* 31 (3), (2016).
- [14] F.G. Turnbull, "Selected harmonic reduction in static dc-ac inverters", *IEEE Trans Communication and Electronics* 83, 374–378 (1964).
- [15] H.S. Patel and R.G. Hoft, "Generalized techniques of harmonic elimination and voltage control in thyristor inverters: part I – harmonic elimination", *IEEE Trans. Industry Applications*, IA-9, 310–317 (1973).
- [16] H.S. Patel and R.G. Hoft, "Generalized techniques of harmonic elimination and voltage control in thyristor inverters: part II – voltage control techniques", *IEEE Trans. Ind. Applications*, IA-10, 666–673 (1974).
- [17] J. Napoles, J.I. Leon, R. Portillo, L.G. Franquelo, and M.A. Aguirre, "Selective harmonic mitigation technique for high-power converters", *IEEE Trans on Ind. Electron.* 57 (7), 2315–2323 (2010).
- [18] M. Steczek and A. Szeląg, "Modification of selective harmonics elimination method for effective catenary current harmonics reduction", *IEEE Int. Conf. Electrical Drives and Power Electronics*, 394–401, Slovakia (2015).
- [19] W. Cong, F. Zhao, X. Guo, X. Wen, Y. Wang, and X. Song, "Analysis and experimental verification for multiple solutions of bipolar SHEPWM waveforms applied in control system of induction machines", *IEEE Int. Conf. on Electrical Machines and Systems*, 1–4 (2011).
- [20] M. Lewandowski and A. Szeląg, "Minimizing harmonics of the output voltage of the chopper inverter", *Archiv für Electrotechnik* 69, 223–226 (1986).
- [21] R.N. Ray, D. Chatterjee, and S.K. Goswami, "An application of PSO technique for harmonic elimination in a PWM inverter", *Applied Soft Computing* (9), 1315–1320 (2009).
- [22] M. Steczek, P. Chudzik, and A. Szeląg, "Combination of SHE and SHM – PWM techniques for VSI DC-link current harmonics control in railway applications", *IEEE Transactions on Industrial Electronics*, Early Access, DOI 10.1109/TIE.2017.2694357 (2017).